Environmental Toxicology and Chemistry—Volume 00, Number 00—pp. 1–7, 2020
Received: 3 June 2020 | Revised: 30 June 2020 | Accepted: 9 November 2020

Environmental Toxicology

Carcinogen-Induced Model of Proangiogenesis in Zebrafish Embryo-Larvae

Nilambari V. Pawar,* Pritee D. Singh, Padmaja S. Prabhu, and Jigarkumar R. Rana

Section of Ecotoxicology, Department of Chemistry, Jai Research Foundation, Valvada, Gujarat, India

Abstract: Tumor angiogenesis is the main target in cancer drug development. Discovery of antiangiogenic agents targeting different mechanisms of action is the major area of research to control tumor growth and metastasis. Zebrafish (in the embryo-larvae stage) acts as an essential preclinical efficacy–toxicity model for antiangiogenic drug discovery. We aimed to develop a carcinogen-induced model of proangiogenesis in zebrafish embryo-larvae using the carcinogens lindane and benzo[*a*]pyrene. Zebrafish were randomly selected for mating. Postspawning, healthy embryos were staged, dispensed in reverse-osmosis water in a 12-well plate, and incubated at 28.5 °C, wherein 24 h postfertilization they were exposed to sublethal concentrations of the carcinogens. Three days postexposure, embryos were stained with alkaline phosphatase, and the angiogenic basket was imaged using a bright-field microscope. The number of subintestinal vessels, their length from somite to the basket, and other proangiogenic parameters were measured and analyzed. The effective concentrations causing a 30% increase in subintestinal vessels for benzo[*a*]pyrene and lindane were 2.69 and 2.24 μM, respectively, thus proving their proangiogenic potency. The carcinogen-induced model of proangiogenesis in zebrafish embryo-larvae can be used as an effective high-throughput screening tool to assess the proangiogenic potential of carcinogenic compounds and to screen antiangiogenic drugs for better therapeutic intervention. *Environ Toxicol Chem* 2020;00:1–7.© 2020 SETAC

Keywords: Carcinogen; Lindane; Benzo[*a*]pyrene; Tumor; Angiogenesis; Zebrafish

INTRODUCTION

Angiogenesis plays a crucial role in the progression, metastatic spread, and vasculature of tumors (Nishida et al. 2006). It supplies oxygen, nutrients, and growth factors constantly to distant tumor sites (Keith and Simon 2008). Reportedly, the most researched angiogenesis-dependent disease is cancer. Although angiogenesis leads to several medical conditions, such as psoriasis, endometriosis, and atherosclerosis, cancer remains the most researched angiogenesis-dependent disease (Folkman 2006; Nussenbaum and Herman 2010). The onset of these diseases from angiogenesis warrants detailed insights into angiogenesis as a whole (Nussenbaum and Herman 2010). Angiogenesis is regulated by molecular pathways associated with endothelial sprouting and nonsprouting microvascular development (Hillen and Griffioen 2007; Fallah et al. 2019). To develop anticancer therapies, targeting of these pathways using a therapeutic approach of drugs and inhibitors is crucial. Thus, in-depth understanding of angiogenesis is necessary for drug discovery and therapeutic advancement (Santoro 2014).

To pursue molecular–pharmacological milestones in cancer research, animal models are preferred to obtain detailed insights into the mechanisms of tumor angiogenesis and testing of antiangiogenic therapies (Santoro 2014). Angiogenic models using rodents and chick embryos have been developed for screening pro- and antiangiogenic compounds (Hasan et al. 2004). However, producing such screening models using higher animals is not often feasible and affordable on a large scale. Tropical teleost zebrafish (*Danio rerio*) is an effective research tool to understand model gene function, organ formation, drug discovery, and toxicology (Khan and Alhewairini 2018). Zebrafish embryo-larvae are preferred over other higher vertebrate animal models because of their low maintenance, optical transparency, high fecundity and fertility, amenability, easy drug administration, rapid embryonic development, and highly characteristic blood-vessel patterning with short developmental period (96 h postfertilization [hpf]; Khan and Alhewairini 2018). Angiogenesis in zebrafish is initiated as early as 12 hpf. By 24 hpf, a simple circulatory loop consisting of major blood vessels is established along with the development of the intersegmental vessels of the trunk. By 24 to 48 hpf,

* Address correspondence to nilambari.pawar@jrfonline.com; nilambari.pawar@gmail.com; jrf@jrfonline.com
Published online 12 November 2020 in Wiley Online Library (wileyonlinelibrary.com).
DOI: 10.1002/etc.4928

subintestinal vessel (SIV)–like angiogenic sprouts develop in the developing gut to establish angiogenesis, allowing evaluation of antiangiogenic agents (Serbedzija et al. 1999; Isogai et al. 2001). Thus, zebrafish helps in effectively understanding tumor angiogenesis and metastasis. Live zebrafish embryos can be administered angiogenic chemicals and drugs to understand the effect of chemicals on survival and migration of malignant cells (Santoro 2014; Tulotta et al. 2016).

The zebrafish efficacy–toxicity model using normal vasculature of zebrafish for antiangiogenic drug discovery has been implemented to screen an array of antiangiogenic compounds with different mechanisms of action for targeting SIVs in zebrafish embryo-larvae and evaluating the model's potency (Chimote et al. 2014). This highlights the potential translational ability of the zebrafish efficacy–toxicity model for antiangiogenic drug discovery and high-throughput screening of angiogenesis.

Physiological angiogenesis is a tightly coordinated process regulated through equilibrium of pro- and antiangiogenic factors, whereas tumor angiogenesis is irregular with unbalanced formation of blood vessels (Cook and Figg 2010). Compared with normal vasculature, tumor-induced vasculature exhibits more profound morphofunctional modifications (Carmeliet and Jain 2000). Thus, animal models with tumor-induced angiogenesis are preferred for effectively screening antiangiogenic compounds and estimating effective concentrations of the drug for reoccurrence of the normal vasculature (Khan and Alhewairini 2018). Tumor angiogenic models have been established in zebrafish as xenografts by transplanting cancer cells in 48-hpf embryo-larvae (Tobia et al. 2011). Although being the best technique, in terms of large-scale screening of new chemical entities, it has certain limitations; the model requires fluorescently tagged human cancer cells, skilled personnel, and a huge number of tumor xenografts. An easy and rapid alternative approach to induce angiogenesis is to use carcinogenic chemicals. Several cancer types have been established in zebrafish using chemicals by adding carcinogens to water, including dibenzo[*a,l*]pyrene, 7,2-dimethylbenz[*a*]anthracene, *N*-dimethylnitrosamine, and *N*-nitrosodiethylamine to develop hepatocarcinoma and *N*-ethyl-*N*-nitrosourea to establish leukemia, melanoma, and testicular cancer (Letrado et al. 2018).

Benzo[*a*]pyrene is the major carcinogen present in tobacco smoke (Li et al. 2010). The compound exhibits both genotoxic and carcinogenic effects. According to the International Agency for Research on Cancer, benzo[*a*]pyrene is a human carcinogen. The compound induces apoptotic and survival signals, both of which are crucial in the development of tumor (Hardonnière et al. 2016). Lindane, an organochlorine insecticide and fumigant, is used in agriculture for seed treatment and against soil-dwelling plant-eating insects. Lindane ranks in the list of ToxCast phase I chemicals and exhibited developmental toxicity in a zebrafish embryo screen with a half-maximal activity concentration of 33.7175 μM (Padilla et al. 2012). It is a neurotoxin that increases the risk of tumor development. Long-term exposure to lindane activates estrogen receptor α and disrupts the endocrine system (Clere et al. 2012). Estrogen receptor α is a key transcription factor and crucial diagnostic–prognostic factor, mainly in breast cancer (Wang et al. 2012). Exposure to benzo[*a*]pyrene and lindane often increases the metastatic potential and invasiveness of tumor cells (Miller et al. 2005; Bharathi et al. 2013). Lindane has been reported to be used to study tumor angiogenesis using ex vivo and in vitro angiogenic models (Bharathi et al. 2013). The proangiogenic ability of lindane has been proved by the development of neovascularization in a chorioallantoic membrane assay (Bharathi et al. 2013). Hence, we aimed to develop a carcinogen-induced model of proangiogenesis in zebrafish embryo-larvae using carcinogens, namely lindane and benzo[*a*]pyrene.

MATERIALS AND METHODS

Materials

Test chemicals for the present study were lindane (Dr. Ehrenstorfer), benzo[*a*]pyrene (Sigma-Aldrich), sorafenib (Clearsynth Labs), and deferoxamine mesylate (Clearsynth Labs). Nitroblue tetrazolium (NBT) chloride–5-bromo-4-chloro-3′-indolyphosphate p-toluidine (BCIP) salt substrate stock solution was purchased from Thermo Fisher Scientific.

Zebrafish

Work on zebrafish was approved by the Institutional Animal Ethics Committee, India, under registration number 35/PO/RcBi/SL/99/CPCSEA. Wild-type zebrafish were maintained in a temperature-controlled room at 26 ± 2 °C with a 16:8-h day:night cycle. Zebrafish were randomly selected for mating and housed in breeding tanks with a male:female ratio of 2:1. Postspawning, embryos were collected from the breeding trap and washed thoroughly to eliminate any debris. These embryos were staged, dispensed in reverse-osmosis water, and maintained at 28.5 °C in an incubator.

Zebrafish angiogenesis assay

Healthy embryos were collected, and same-stage embryos were kept in reverse-osmosis water in a 12-well plate with each well containing 12 embryos. Embryos were incubated at 28.5 °C for 24 h. At 24 hpf, embryos were exposed to the test chemicals, with each concentration of test chemical containing 12 embryos. The antiangiogenic compound sorafenib and the proangiogenic compound deferoxamine mesylate were used as positive controls (Food and Drug Administration 2007; El-Serag 2017). Deferoxamine mesylate is known to trigger angiogenesis via vascular endothelial cell function (Ikeda et al. 2011). Sorafenib is a targeted drug used for treating tumors. It is a multikinase inhibitor with potent antiangiogenic activity (Pignochino et al. 2009). Test concentrations selected for sorafenib were 0.1, 0.25, 0.5, and 1.0 μM based on the results of Chimote et al. (2014). Concentrations of deferoxamine mesylate were 25, 50, 100, and 200 μM (Hamilton et al. 2014; Wahl et al. 2016). Test concentrations for benzo[*a*]pyrene were 0.0 (control), 2.5, 5.0, 10.0, and 20.0 μM;

and those for lindane were 0.0 (control), 1.56, 3.125, 6.25, and 12.5 μM based on a previous range-finding study conducted (data not included). Stock solutions for all test chemicals were prepared in dimethyl sulfoxide (DMSO) as a solubilizing agent, and hence, a solvent control with a final concentration of 0.1% DMSO was included. All test concentrations were made in reverse-osmosis water containing 0.003% (w/v) phenyl-thiourea for depigmentation and bath-applied to zebrafish embryos. Posttreatment, embryo-larvae were incubated at 28.5 °C for up to 96 hpf (4 d). On day 4, alkaline phosphatase staining was performed by a set procedure (Nusslein-Volhard and Dahm 2002). Experimental larvae were fixed with paraformaldehyde for 30 min at room temperature, followed by dehydration using chilled acetone (30 min at −20 °C). Larvae were washed thrice with washing buffer (10 × phosphate-buffered saline + 10% Tween 20), followed by staining buffer (NTMT: 5 M NaCl + 1 M Tris [pH 9.0–9.5] + 1 M magnesium chloride + 10% Tween 20). Staining solution (NTMT buffer + NBT-BCIP substrate in a ratio of 1:1) was added, and larvae were incubated in the dark at room temperature for 30 min or until the angiogenic basket was stained. Once stained, the larvae were washed twice with washing buffer, followed by equilibration with 50% glycerol and 87% glycerol. Larvae were then stored in glycerol at 4 °C until the next use.

Imaging and scoring of parameters

Stained larvae were imaged using a bright field microscope, focusing on the angiogenic basket. An individual larva was carefully mounted in mounting medium (87% glycerol) on a cavity slide using Pasteur pipette and positioned on its lateral side to get the best view of the angiogenic basket. Images were captured for all the stained larvae. As depicted in Figure 1, the angiogenic parameters (number of SIVs and their length from somite to the angiogenic basket) were evaluated in each larva using ImageJ software, and proangiogenic parameters, such as out-branching, internal bifurcation, and basket distortion, were scored. Using this information, percentage increases in angiogenic and proangiogenic parameters were calculated for deferoxamine mesylate, benzo[*a*]pyrene, and lindane compared to control (Figures 2 and 3). Percentage of inhibition of angiogenic parameters was calculated for sorafenib (Figure 2).

Statistical analysis

One-way analysis of variance and Dunnett's multiple comparison tests were used for calculating significant differences in number of SIVs and length of the angiogenic basket (angiogenic parameters) between the treatment and control groups. Fisher's exact test was applied for statistical significance of proangiogenic factors between the treatment and control in the benzo[*a*]pyrene, lindane, and deferoxamine mesylate groups. $p \leq 0.05$ was considered statistically significant. Finney's method of probit analysis was used to determine 30% effective concentration values (EC30).

RESULTS AND DISCUSSION

Because sublethal concentrations of the 4 test chemicals were used for treatment, all treated larvae were alive at

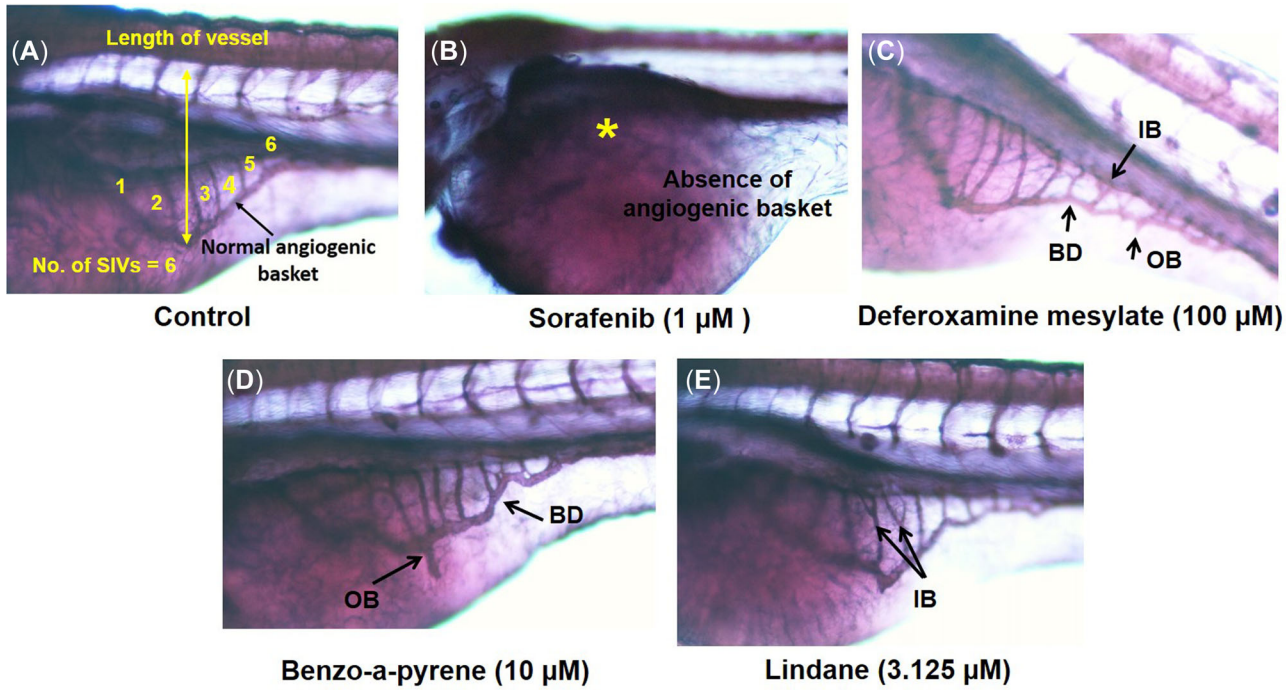

FIGURE 1: Alkaline phosphatase staining. Normal angiogenic basket in control showing scoring of angiogenic parameters (**A**); sorafenib, anti-angiogenic positive control (**B**); proangiogenic parameters out-branching, internal bifurcation, and basket distortion for deferoxamine mesylate (proangiogenic positive control) (**C**); benzo[*a*]pyrene (**D**); and lindane (**E**). BD = basket distortion; IB = internal bifurcation; OB = out-branching; SIV = subintestinal vessel.

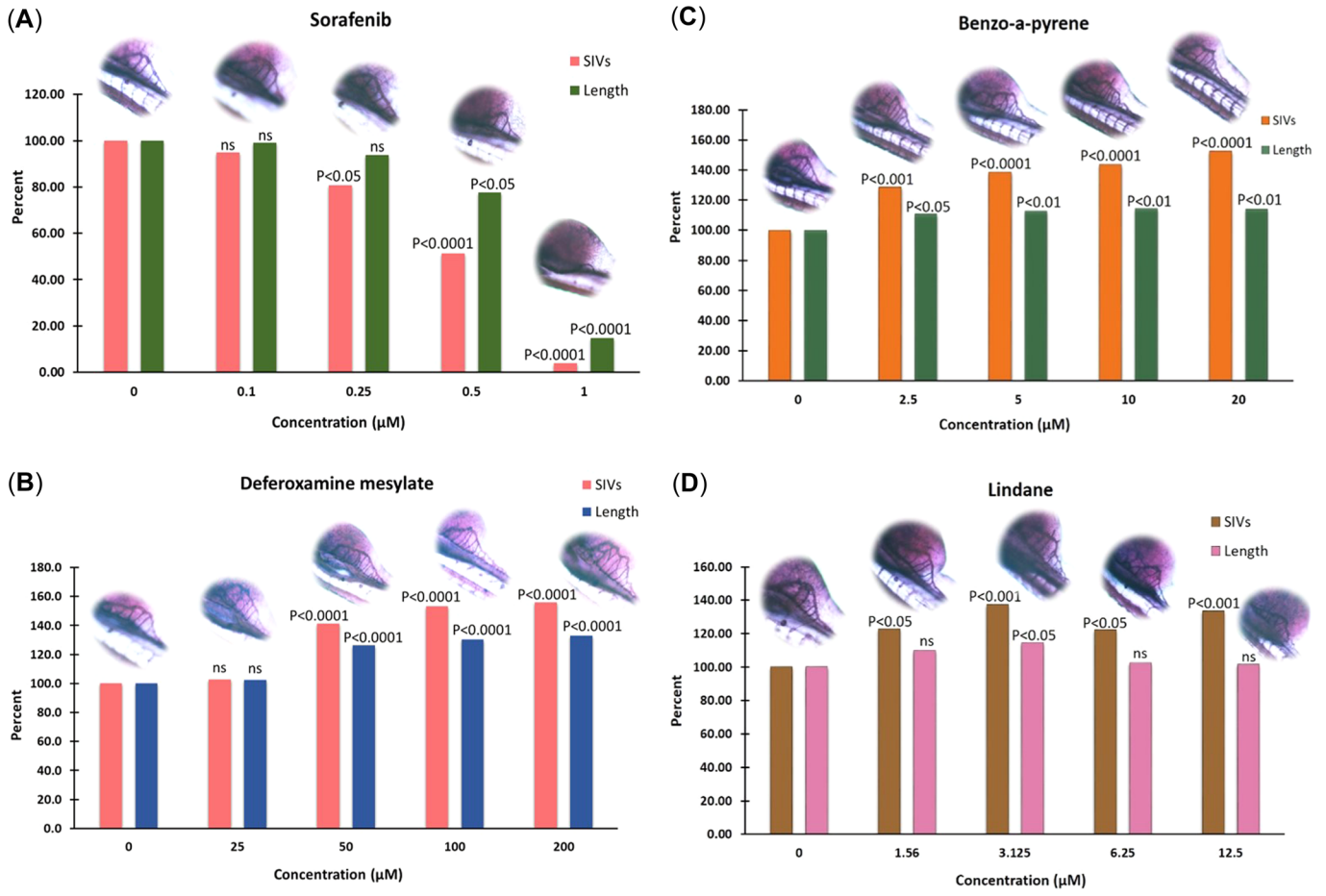

FIGURE 2: Percentage of subintestinal vessels and angiogenic basket length on exposure to sorafenib (**A**), deferoxamine mesylate (**B**), benzo[*a*]pyrene (**C**), and lindane (**D**). ns = not significant; SIV = subintestinal vessel.

treatment termination (96 hpf) and prior to alkaline phosphatase staining. The final concentrations of DMSO (0.1%) and phenyl-thiourea (0.003%) used in the present study were safe and had no influence on the morphology of zebrafish embryos (Karlsson et al. 2001; Hamilton et al. 2014). All calculations were performed comparing the treatment with the solvent control group, hereafter referred to as "control." Larvae in benzo[*a*]pyrene and deferoxamine mesylate did not exhibit any malformations or overt toxicities at any of the test concentrations. Pericardial edema was observed in larvae exposed at 1 µM sorafenib, which is comparable to the off-target effect observed by Chimote et al. (2014). Larvae treated with lindane showed scoliosis at 6.25 and 12.5 µM concentrations. Angiogenic parameters were evaluated for all the test chemicals as percentage increase or decrease in number of SIVs and vessel length compared to the control normalized to 100% (Figure 2). Poststaining, all 12 larvae in the control and all the treatment groups of sorafenib and deferoxamine mesylate were imaged and scored for angiogenic parameters. One larva at 2.5 µM benzo[*a*]pyrene and another at 6.25 µM lindane were damaged during handling; hence, 11 larvae were imaged and scored for these concentrations, and for the rest all concentrations consisted of 12 larvae. Angiogenic parameters showed a concentration-dependent trend for all test chemicals, at all concentrations, except at the 2 higher concentrations for lindane (Figure 2). Proangiogenic parameters for deferoxamine mesylate, benzo[*a*]pyrene, and lindane were scored as count data (i.e., the number of larvae showing the effect of the total larvae imaged), presented as percentage increases in outbranching, internal bifurcation, and basket distortion compared to the control normalized to 0% (Figure 3). Proangiogenic parameters showed concentration-dependent increases for deferoxamine mesylate, benzo[*a*]pyrene, and lindane at all concentrations, except at the 2 higher concentrations for lindane (Figure 3). Systemic toxicity observed in treated larvae at the 2 higher concentrations for lindane (6.25 and 12.5 µM) might have affected the angiogenic and proangiogenic parameters at these 2 concentrations.

The anti- or proangiogenic efficacy of each test chemical was determined from its concentration–response model for change in the number of SIVs by calculating the effective concentration. The effective concentration (EC30) was defined as the test concentration leading to a 30% change in the number of SIVs compared with the mean SIVs for the control. Number of SIVs was a preferred parameter, and determination of EC30 was considered because it could be calculated for all the test

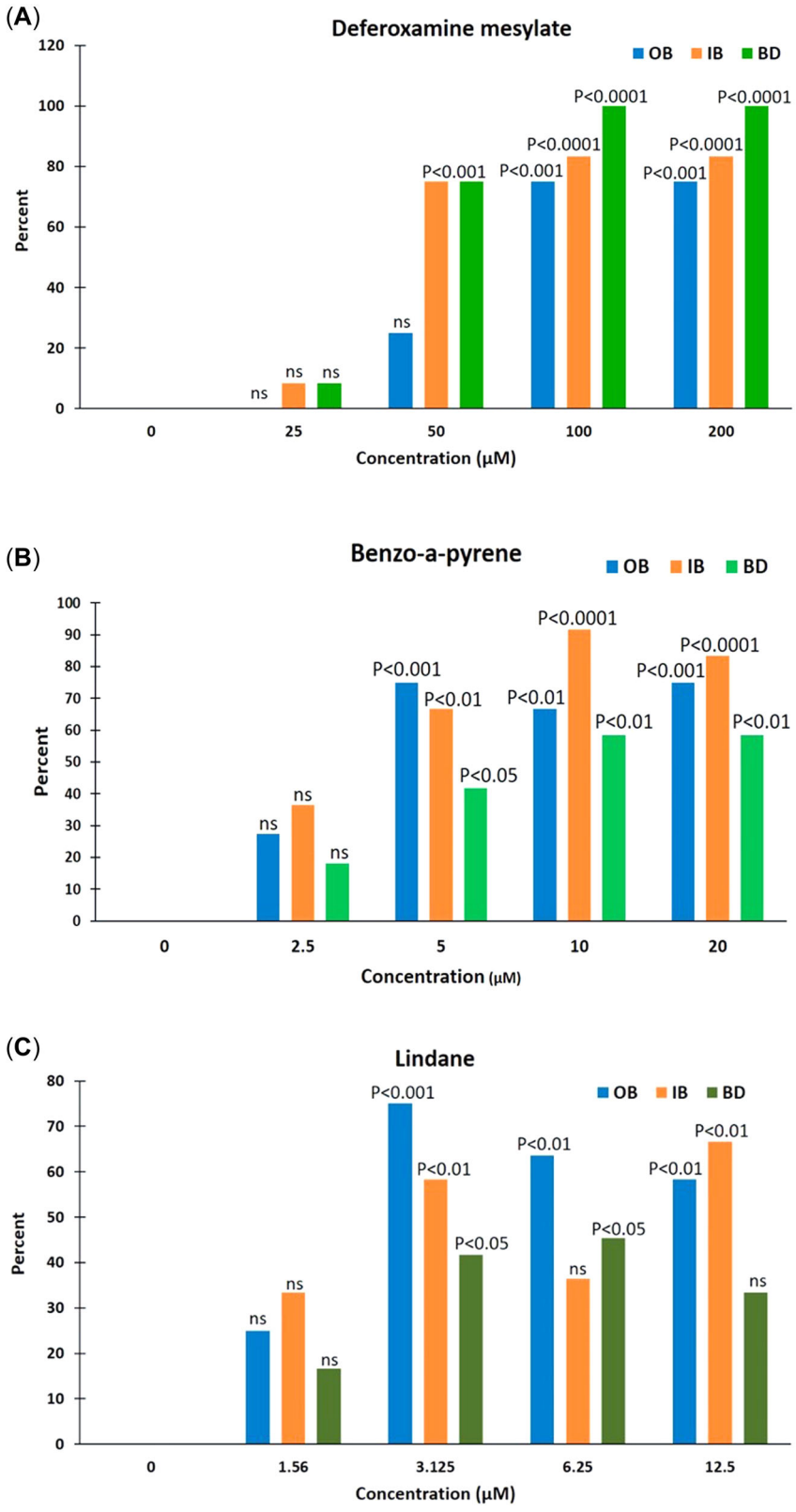

FIGURE 3: Percentage of proangiogenic parameters for deferoxamine mesylate (**A**), benzo[*a*]pyrene (**B**), and lindane (**C**). BD = basket distortion; IB = internal bifurcation; OB = out-branching.

TABLE 1: Comparison of lowest-observed-effect concentration, median lethal concentration, and effective concentration causing 30% change in subintestinal vessels of test chemicals

Test chemical	Bioactivity	LOEC (μM)	LC50 (μM)	EC30 (μM)
Sorafenib	Antiangiogenic positive control	1.0[a]	2.0 ± 0.09[a]	0.30
Deferoxamine mesylate	Proangiogenic positive control	—	>1000[b]	55.8
Benzo[a]pyrene	Carcinogen	—	>20	2.69
Lindane	Carcinogen	6.25	>12.5	2.24

[a]Chimote et al. (2014).
[b]Hamilton et al. (2014).
— = not applicable; EC30 = effective concentration causing 30% change in subintestinal vessels; LC50 = median lethal concentration; LOEC = lowest-observed-effect concentration.

chemicals. All the concentrations of sorafenib, deferoxamine mesylate, and benzo[*a*]pyrene were used for the effective concentration calculation. For lindane, only the 2 lower-concentration groups showing the concentration–response model were used. The EC30 for sorafenib was 0.30 μM, leading to 30% inhibition of SIVs. The EC30s for deferoxamine mesylate, benzo[*a*]pyrene, and lindane were 55.8, 2.69, and 2.24 μM, respectively, leading to 30% increases of SIVs (Table 1).

Based on the previous range-finding study conducted (data not included), the median lethal concentrations (LC50) of benzo[*a*]pyrene and lindane were >20 and >12.5 μM, respectively. Higher concentrations were not tested because they precipitated in reverse-osmosis water. Table 1 compares the lowest-observed-effect concentration, the LC50, and the EC30 of test chemicals. The calculated EC30 was less than the LC50 for the test carcinogens as well as for the 2 positive chemicals. Compared to the concentration level of 20 mg/L (~69 μM) lindane required for stimulating angiogenesis in the chorioallantoic membrane assay (Bharathi et al. 2013) and approximately 4 μM of benzo[*a*]pyrene needed to increase the metastatic potential and invasiveness of MDA-MB-231 cells (Miller et al. 2005), our zebrafish model exhibited angiogenesis stimulation at an effective concentration of 2.24 μM for lindane and 2.69 μM for benzo[*a*]pyrene, with a 30% increase in SIVs. This proves the greater potency of the 2 test carcinogens to induce proangiogenesis in the zebrafish embryo-larvae model at safe concentrations without interference of any other systemic toxicities or malformations.

A carcinogen-induced tumor model is an easy and rapid alternative to develop proangiogenesis, and hence, this approach was used in the present study. Although chemical carcinogenesis is known to exhibit late onset and low incidence of tumor formation (Stoletov and Klemke 2008), we observed the effect on the angiogenic basket in zebrafish within only 3 d postexposure to lindane and benzo[*a*]pyrene and with the 2 positive compounds. This might be due to the selection of the developmental stage in zebrafish. Tumor development is more rapid in embryos than in adults. Moreover, embryos have the advantage of transparent bodies that allow easy microscopic observation (Letrado et al. 2018). The sensitivity of our test organism, zebrafish embryo-larvae, for the angiogenesis assay was evaluated using 2 positive test chemicals, deferoxamine mesylate and sorafenib.

The present study suggests that zebrafish is an effective means to better understand tumor angiogenesis in vivo; this can proffer new insights into the development of therapeutic approaches, tumor progression, and patient outcome. Moreover, the present study proposes that a proangiogenesis screening zebrafish model can potentially complement higher animal models, provide details on the molecular mechanism of tumor angiogenesis, and provide a high-throughput screening platform.

The findings of the present study indicate that benzo[*a*]pyrene and lindane exhibit proangiogenesis, which is evident by their potential to disrupt the angiogenic basket, giving rise to outward and internal branching of the vessels as observed when injected with tumor cells by Moshal et al. (2011); thus, the effective concentration can be used to develop a proangiogenic model. High-throughput screening of angiogenesis using zebrafish can evaluate and compare anti- and proangiogenic activities of tumor cells on the basis of a carcinogen-induced neovascular response of the developing SIVs (Moshal et al. 2011).

A large number of zebrafish embryos can be transplanted, and they are permeable to small molecules, because of which screening of angiogenesis using zebrafish is gaining attention; it is being tested and validated for multiple antiangiogenic molecules (Moshal et al. 2011). Nevertheless, establishing a large-scale quantitative in vivo assay for measuring tumor-induced angiogenesis is highly required (Moshal et al. 2011). With respect to this, the present study suggests considering the number and length of the vessels as well as the formation of the angiogenic basket as reliable, consistent parameters for quantifying tumor angiogenesis in zebrafish embryo-larvae.

This zebrafish model of proangiogenesis can be employed as a high-throughput screening tool for a dual purpose: 1) to screen for proangiogenic/carcinogenic potential of compounds, resulting in the selection of safer compounds entering the agricultural market and cancer risk assessment of harmful pollutants, and 2) to screen for potential antiangiogenic compounds in cancer drug discovery.

CONCLUSION

The results of the present study successfully demonstrate the development of a proangiogenic model of zebrafish using lindane and benzo[*a*]pyrene. This zebrafish model of proangiogenesis can be employed to screen an array of compounds with proangiogenic/carcinogenic potential. A carcinogen-induced proangiogenic model can also be used to screen for potential antiangiogenic compounds in cancer drug discovery. This model can further be explored for identifying the specific type of cancer developed by the carcinogens so as to be used as an efficacy model to screen new chemical entities targeting specific cancer types. This will help to speed up the early preclinical drug discovery process by minimizing the use of higher animals, time, and cost.

Disclaimer—The authors declare that there is no conflict of interest.

Author Contributions Statement—N.V. Pawar and J.R. Rana: study conception and design; N.V. Pawar: definition of intellectual content, performance of experimental study, data analysis, literature review, writing and editing the manuscript; P.D. Singh: breeding setup and embryo collection; N.V. Pawar, J.R. Rana, and P.S. Prabhu: manuscript review.

Data Availability Statement—Data, associated metadata, and calculation tools are available from the corresponding author (nilambari.pawar@jrfonline.com, nilambari.pawar@gmail.com, jrf@jrfonline.com).

REFERENCES

Bharathi SP, Raj HM, Jain S, Banerjee BD, Ahmed T, Arora VK. 2013. Role of pesticides in the induction of tumor angiogenesis. *Anticancer Res* 33:231–240.

Carmeliet P, Jain RK. 2000. Angiogenesis in cancer and other diseases. *Nature* 407:249–257.

Chimote G, Sreenivasan J, Pawar N, Subramanian J, Sivaramakrishnan H, Sharma S. 2014. Comparison of effects of anti-angiogenic agents in the zebrafish efficacy–toxicity model for translational anti-angiogenic drug discovery. *Drug Des Devel Ther* 8:1107–1123.

Clere N, Lauret E, Malthiery Y, Andriantsitohaina R, Faure S. 2012. Estrogen receptor alpha as a key target of organochlorines to promote angiogenesis. *Angiogenesis* 15:745–760.

Cook KM, Figg WD. 2010. Angiogenesis inhibitors: Current strategies and future prospects. *CA Cancer J Clin* 60:222–243.

El-Serag HB. 2017. Current status of sorafenib use for treatment of hepatocellular carcinoma. *Gastroenterol Hepatol (NY)* 13:623–625.

Fallah A, Sadeghinia A, Kahroba H, Samadi A, Heidari HR, Bradaran B, Zeinali S, Molavi O. 2019. Therapeutic targeting of angiogenesis molecular pathways in angiogenesis-dependent diseases. *Biomed Pharmacother* 110:775–785.

Folkman J. 2006. Angiogenesis. *Annu Rev Med* 57:1–8.

Food and Drug Administration. 2007. FDA approves nexavar for patients with inoperable liver cancer. Press release, November 19. Silver Spring, Maryland, USA.

Hamilton JL, Hatef A, Imran ul-haq M, Nair N, Unniappan S, Kizhakkedathu JN. 2014. Clinically approved iron chelators influence zebrafish mortality, hatching morphology and cardiac function. *PLoS One* 9:e109880.

Hardonnière K, Saunier E, Lemarié A, Fernier M, Gallais I, Héliès-Toussaint C, Mograbi B, Antonio S, Bénit P, Rustin P, Janin M. 2016. The environmental carcinogen benzo[a]pyrene induces a Warburg-like metabolic reprogramming dependent on NHE1 and associated with cell survival. *Sci Rep* 6:30776.

Hasan J, Shnyder SD, Bibby M, Double JA, Bicknel R, Jayson GC. 2004. Quantitative angiogenesis assays in vivo—A review. *Angiogenesis* 7:1–16.

Hillen F, Griffioen AW. 2007. Tumour vascularization: Sprouting angiogenesis and beyond. *Cancer Metastasis Rev* 26:489–502.

Ikeda Y, Tajima S, Yoshida S, Yamano N, Kihira Y, Ishizawa K, Aihara KI, Tomita S, Tsuchiya K, Tamaki T. 2011. Deferoxamine promotes angiogenesis via the activation of vascular endothelial cell function. *Atherosclerosis* 215:339–347.

Isogai S, Horiguchi M, Weinstein BM. 2001. The vascular anatomy of the developing zebrafish: An atlas of embryonic and early larval development. *Dev Biol* 230:278–301.

Karlsson J, von Hofsten J, Olsson PE. 2001. Generating transparent zebrafish: A refined method to improve detection of gene expression during embryonic development. *Mar Biotechnol* 3:522–527.

Keith B, Simon MC. 2008. Tumor angiogenesis. In Mendelson J, Howley P, Israel MA, Gray JW, Thompson CB, eds, *Molecular Basis of Cancer*, 8th ed. Saunders, Philadelphia, PA, USA, pp 241–252.

Khan FR, Alhewairini SS. 2018. Zebrafish (*Danio rerio*) as a model organism. In Streba L, ed, *Current Trends in Cancer Management*. IntechOpen, London, UK, pp 3–18.

Letrado P, de Miguel I, Lamberto I, Díez-Martínez R, Oyarzabal J. 2018. Zebrafish: Speeding up the cancer drug discovery process. *Cancer Res* 78:6048–6058.

Li CH, Cheng YW, Hsu YT, Hsu YJ, Liao PL, Kang JJ. 2010. Benzo[*a*]pyrene inhibits angiogenic factors–induced alphavbeta3 integrin expression, neovasculogenesis, and angiogenesis in human umbilical vein endothelial cells. *Toxicol Sci* 118:544–553.

Miller ME, Holloway AC, Foster WG. 2005. Benzo-[*a*]-pyrene increases invasion in MDA-MB-231 breast cancer cells via increased COX-II expression and prostaglandin E 2 (PGE 2) output. *Clin Exp Metastasis* 22:149–156.

Moshal KS, Ferri-Lagneau KF, Haider J, Pardhanani P, Leung T. 2011. Discriminating different cancer cells using a zebrafish in vivo assay. *Cancers* 3:4102–4013.

Nishida N, Yano H, Nishida T, Kamura T, Kojiro M. 2006. Angiogenesis in cancer. *Vasc Health Risk Manag* 2:213–219.

Nussenbaum F, Herman IM. 2010. Tumor angiogenesis: Insights and innovations. *J Oncol* 2010:132641.

Nusslein-Volhard C, Dahm R, eds. 2002. *Zebrafish: A Practical Approach*. Oxford University Press, Oxford, UK.

Padilla S, Corum D, Padnos B, Hunter DL, Beam A, Houck KA, Sipes N, Kleinstreuer N, Knudsen T, Dix DJ, Reif DM. 2012. Zebrafish developmental screening of the ToxCast™ phase I chemical library. *Reprod Toxicol* 33:174–187.

Pignochino Y, Grignani G, Cavalloni G, Motta M, Tapparo M, Bruno S, Bottos A, Gammaitoni L, Migliardi G, Camussi G, Alberghini M. 2009. Sorafenib blocks tumour growth, angiogenesis and metastatic potential in preclinical models of osteosarcoma through a mechanism potentially involving the inhibition of ERK1/2, MCL-1 and ezrin pathways. *Mol Cancer* 8:118.

Santoro MM. 2014. Antiangiogenic cancer drug using the zebrafish model. *Arterioscler Thromb Vasc Biol* 34:1846–1853.

Serbedzija GN, Flynn E, Willett CE. 1999. Zebrafish angiogenesis: A new model for drug screening. *Angiogenesis* 3:353–359.

Stoletov K, Klemke R. 2008. Catch of the day: Zebrafish as a human cancer model. *Oncogene* 27:4509–4521.

Tobia C, De Sena G, Presta M. 2011. Zebrafish embryo, a tool to study tumour angiogenesis. *Int J Dev Biol* 55:505–509.

Tulotta C, He S, Van Der Ent W, Chen L, Groenewoud A, Spaink HP, Snaar-Jagalska BE. 2016. Imaging cancer angiogenesis and metastasis in a zebrafish embryo model. In Langenau DM, ed, *Cancer and Zebrafish: Mechanisms, Techniques, and Models*. Springer, Cham, Switzerland, pp 239–263.

Wahl EA, Schenck TL, Machens HG, Balmayor ER. 2016. VEGF released by deferoxamine preconditioned mesenchymal stem cells seeded on collagen-GAG substrates enhances neovascularization. *Sci Rep* 6:36879.

Wang D, Huang P, Zhu B, Sun L, Huang Q, Wang J. 2012. Induction of estrogen receptor a-36 expression by bone morphogenetic protein 2 in breast cancer cell lines. *Mol Med Rep* 6:591–596.

